Microfluid Nanofluid (2010) 9:17–30
DOI 10.1007/s10404-009-0508-4

RESEARCH PAPER

Decreasing microfluidic evaporation loss using the HMDL method: open systems for nucleic acid amplification and analysis

Chunsun Zhang · Da Xing

Received: 6 July 2009 / Accepted: 9 September 2009 / Published online: 20 October 2009

Abstract Evaporation is of great importance when dealing with microfluidic devices with open air/liquid interfaces due to the large surface-to-volume ratio. For devices utilizing a thermal reaction (TR) reservoir to perform a series of biological and chemical reactions, excessive heat-induced microfluidic evaporation can quickly lead to reaction reservoir dry out and failure of the overall device. In this study, we present a simple, novel method to decrease heat-induced fluid evaporation within microfluidic systems, which is termed as heat-mediated diffusion-limited (HMDL) method. This method does not need complicated thermal isolation to reduce the interfacial temperature, or external pure water to be added continuously to the TR chamber to compensate for evaporation loss. The principle of the HMDL method is to make use of the evaporated reaction content to increase the vapor concentration in the diffusion channel. The experimental results have shown that the relative evaporation loss (V_{loss}/V_{ini}) based on the HMDL method is not only dependent on the HMDL and TR region's temperatures (T_{HMDL} and T_{TR}), but also on the HMDL and TR's channel geometries. Using the U-shaped uniform channel with a diameter of 200 μm, the V_{loss}/V_{ini} within 60 min is low to 5% ($T_{HMDL} = 105°C$, $T_{TR} = 95°C$). The HMDL method can be used to design open microfluidic systems for nucleic acid amplification and analysis such as isothermal amplification and PCR thermocycling amplification, and a PCR process has been demonstrated by amplifying a 135-bp fragment from *Listeria monocytogenes* genomic DNA.

Keywords Microfluidic evaporation loss · Heat-mediated diffusion-limited (HMDL) · Open microfluidic systems · Polymerase chain reaction · Genetic amplification and analysis

C. Zhang · D. Xing (✉)
MOE Key Laboratory of Laser Life Science and Institute of Laser Life Science, College of Biophotonics, South China Normal University, No.55, Zhongshan Avenue West, Tianhe District, 510631 Guangzhou, People's Republic of China
e-mail: xingda@scnu.edu.cn

1 Introduction

Temperature is no doubt the often used parameter in macro-, micro-, and nano-fluidic systems (Squires and Quake 2005). Many reactors for biochemical analysis are temperature-controlled and require relatively high operating temperatures, such as the temperature cycling reactions including polymerase chain reaction (PCR) (~94, ~55, ~72°C) (Saiki et al. 1985), Sanger DNA sequencing (~95, ~55, ~60°C) (Blazej et al. 2006), allele-specific ligase chain reaction (LCR) and ligase detection reaction (LDR) (~94, ~60°C) (Hashimoto et al. 2006), and the isothermal reactions including the multiple-strand displacement amplification (MDA) (30°C) (Marcy et al. 2007; Michikawa et al. 2008), rolling circle amplification (RCA) (30–37°C) (Ericsson et al. 2008; Hutchison et al. 2005), nucleic acid sequence-based amplification (NASBA) (41°C) (Dimov et al. 2008; Gulliksen et al. 2004; Morisset et al. 2008), loop-mediated isothermal amplification (LAMP) (60–65°C) (Lam et al. 2008), padlock ligation reaction (50°C) (Ericsson et al. 2008), enzyme digestion reaction (37°C) (Ericsson et al. 2008), and reverse transcription reaction (42–50°C) (VanDijken et al. 2007). These biochemical assays have been performed in either bench or microfluidic thermocyclers, and have witnessed many potential applications.

During the past several years, microfluidics technologies have enabled the development of rapid and inexpensive bioreaction systems. A bioreaction microsystem offers several advantages, including reduced reagent costs and the amount of chemical waste, decreased reaction time, reduced risk of contamination, simplified liquid handling, and high integration. In general, there are two kinds of miniaturized PCR systems (Zhang et al. 2006; Zhang and Xing 2007), a steady fluid PCR (Cho et al. 2006; Easley et al. 2006; Guttenberg et al. 2005; Legendre et al. 2006; Matsubara et al. 2005; Neuzil et al. 2006; Oh et al. 2005; Pal et al. 2005; Pilarski et al. 2005; Prakash et al. 2006; Toriello et al. 2008), and a dynamic flow PCR (Cheng et al. 2005; Hashimoto et al. 2006; Kopp et al. 1998; Sista et al. 2008). For these two categories of miniaturized systems, recent trends turn to integrate bioreactors with sample preparation, fluidic handling, and product detection to produce micro total analytical systems (μTAS) (Easley et al. 2006; Sista et al. 2008; Toriello et al. 2008).

One of the well-known issues using miniaturized bioreaction systems is evaporation at the open air–liquid interfaces (Berthier et al. 2008a, b; Lynn et al. 2009; Eijkel and van den Berg 2005). Evaporation can be put to good use by employing it as a microfluidic pumping (Effenhauser et al. 2002; Goedecke et al. 2002; Heuck et al. 2008; Namasivayam et al. 2003; Zimmermann et al. 2005; Xu et al. 2008) or sample concentration (Timmer et al. 2003; Walker and Beebe 2002) mechanism. However, evaporation is also seen as a problematic issue for most applications, especially for temperature-controlled small-scale bioreaction systems. If no action is taken to replenish the solvents being evaporated in these systems, sub-microliter-sized volumes can dry out within a few minutes, requiring a sufficiently fast analytical procedure (Neugebauer et al. 2004). There are many approaches to preventing or reducing heat-induced microfluidic evaporation loss during heating or thermocycling. A straightforward and frequently used approach is to block any open gas–liquid interface. An immiscible liquid is typically used to cap the exposed reaction solutions, such as mineral oil (Easley et al. 2006; Guttenberg et al. 2005; Legendre et al. 2006; Matsubara et al. 2005; Neuzil et al. 2006; Sista et al. 2008; Bratten et al. 1997) or another organic liquid (for example octane) (Litborn and Roeraade 2000). The non-miscible mineral oil is a suitable liquid cover preventing evaporation of the underlying solution because it has a boiling point far above 100°C and a density slightly below 1.0 g/cm^3. However, the use of viscous mineral oil would complicate fluid of interest and accurate dispensing of nanoliter or picoliter volumes. In addition, this approach will also increase the risk of cross contamination. Much akin to mineral oil, wax can also be used to cover the inlet/outlet holes of reaction chamber to avoid evaporation of the sample (Gulliksen et al. 2004). Another approach is to use microvalves or solid lids to seal the reaction chamber (Moerman et al. 2005; Cheng et al. 2005; Cho et al. 2006; Oh et al. 2005; Pal et al. 2005; Pilarski et al. 2005; Prakash et al. 2006; Toriello et al. 2006, 2008). It is common knowledge that the evaporation rate reduces with increase of the gas pressure around a liquid. However, because all microvalves require some kind of physical confinement and most need to provide some kind of actuations to operate, they often add to the complexity of the fabrication and fluidic handling (Zhang et al. 2007). Other approaches can also be utilized to mitigate evaporation. For example, evaporation can be suppressed by directly placing the microfluidic device in a sealed humid environment (Litborn et al. 1999, 2000). This involves control of the relative humidity directly above the air/liquid interface, usually performed through sample placement near a water bath to keep the surrounding air saturated with water vapor. However, this approach is typically empirical and relies on the assumption that the level of humidity provided is sufficient to alleviate evaporation. In addition, as microfluidic devices become denser and use specialized equipment with space constraints, it is impossible to deposit liquid in the same manner and a design parameter to ensure acceptable evaporation is often needed (Berthier et al. 2008a, b). More complicated approaches involve the fabrication of reservoir arrays from agarose gel (Minarik et al. 2002). These gel arrays are made of over 90% water, saturating the local environment above each well and greatly minimizing the evaporation.

Simple microfluidic devices are often open or unsealed systems to ease the introduction and/or the withdrawal of reaction fluids. Therefore, a simple approach to reduce the evaporation loss without covers, microvalves, or sacrificial water is highly desirable for microfluidic reaction applications. In this article, we report on a simple, novel method to decrease heat-induced fluid evaporation within microfluidic systems, which is termed as heat-mediated diffusion-limited (HMDL) method. The underlying principle of this method is to make the most of the evaporated reaction content to increase the vapor concentration in the diffusion channel. Therefore, the HMDL method per se is a self-contained vapor replenishment methodology to decrease heat-induced microfluidic evaporation loss.

2 Materials and methods

2.1 Principle of design for the HMDL method

The principle of the HMDL method is based on the concept of diffusion-limited (DL) evaporation. Within our initial experiments, the volume of liquid in the open thermal

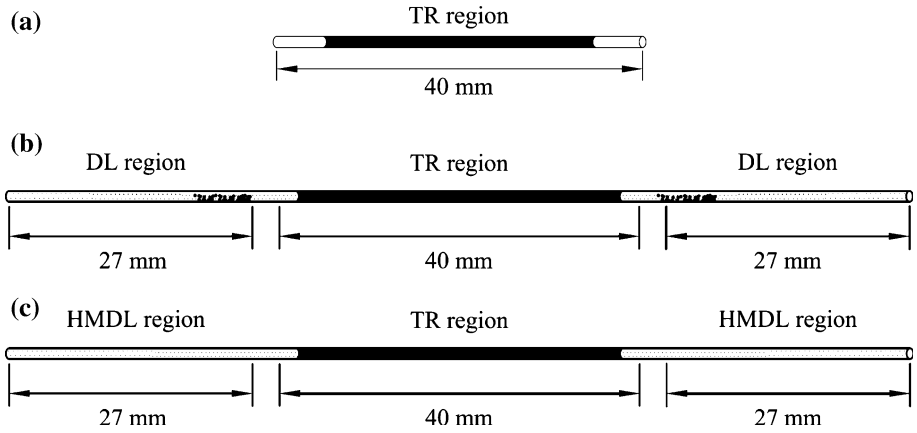

Fig. 1 Schematic diagram of the HMDL method decreasing the heat-induced microfluidic evaporation. **a** Only TR region without DL or HMDL region. **b** TR region with the long-armed DL region which is exposed to the natural environment. **c** TR region with the long-armed HMDL region. *HMDL* heat-mediated diffusion-limited, *TR* thermal reaction, *DL* diffusion-limited

reaction (TR) reservoir without DL region (Fig. 1a) can greatly reduce or dry out within a few minutes when it is exposed to the enhanced temperature condition (for example 95°C for the denaturation of double-stranded DNA). This uncontrolled evaporation can lead to unwanted changes to the initial experimental conditions and, if given enough time, failure of the microfluidic device. And then, the long-armed DL regions, which are exposed to the nature environment, are engrafted onto the TR region (Fig. 1b). Although this approach can reduce the microfluidic evaporation loss to a certain extent, condensation occurs within the DL regions, usually done by bringing the vapor into contact with a solid surface whose temperature is below the saturation temperature of the vapor. At the place adjacent to the TR region, the amount of the condensate liquid increases with time and the liquid 'plug' will form within the microchannel. As a result, the air gap forms between the liquid plug and the TR liquid. However, this air gap has an adverse effect on the steady flow PCR thermal cycling. When the DL regions are subjected to elevated temperatures (Fig. 1c), which is termed as the HMDL method, this adverse effect can be completely circumvented, while the heat-induced evaporation loss is effectively reduced.

In the design, the HMDL channels (input and output) to the heated TR channel provide a resistance that reduces the evaporation rate from the reaction fluid. Vapor that evaporates from the reaction liquid meniscus must diffuse through the HMDL microchannels before it can escape into the natural environment. The rate of evaporation is limited by this vapor diffusion rate. The HMDL evaporation rate can be evaluated from the mass transfer equations. Written in terms of D_v, the diffusivity of water vapor in air, ρ_w, the density of water, C, the mass concentration of water vapor (kg/m^3), and $\vec{n}$, the unit vector normal to the interface, the evaporation rate, E, is given by: $E = \frac{D_v}{\rho_w}\int \frac{\delta C}{\delta \vec{n}} dS$ (Berthier et al. 2008a). For a three-step PCR thermocycling reaction, Wang et al. (2008) have recently proposed a relation expression for the total evaporative volume loss during a DL evaporation process (V_{loss}) : $V_{loss} = 2A_c\left(\sqrt{n\sum_{j=1}^{3}\frac{2PM_wD_{vj}t_{Fj}}{\rho_w RT_{ij}}\ln\left(\frac{P-p_0}{P-p_{vj}}\right)+x_0^2}-x_0\right)$, where A_c is the cross-section area of the diffusion channel, n is the number of cycles, P is the atmosphere pressure, M_w is the molecular weight of water, R is the ideal gas constant, T_{ij}, p_{vj}, t_{Fj} and D_{vj} are the liquid interfacial temperature, vapor pressure, reaction time, and vapor diffusivity at different thermocycling steps, respectively, p_0 is the ambient vapor pressure and x_0 is the initial diffusion length. From this equation, the variables that we can adjust to decrease V_{loss} mainly are the initial diffusion length x_0, the channel cross-section area A_c, and the liquid interfacial temperature T_{ij}. The temperature near the liquid interface also determines the interfacial vapor pressure p_{vj} and the vapor diffusivity D_{vj}. Variables such as n, t_{Fj}, M_w, and ρ_w are determined by the reaction protocols, and p_0 is negligible compared to the atmosphere pressure P. In this study, the topic is restricted to experimental studies concerning the controlled heat-induced microfluidic evaporation loss using the HMDL method, with the focus on those experiments from the constant initial diffusion length x_0.

2.2 Description of device design and instrumentation

The experiments were performed using a computer-controlled, LabView-based temperature control and measure system developed in our laboratory (Zhang and Xing 2009). A schematic of the equipment is shown in Fig. 2 and the setup mainly consists of the following parts: three grooved copper heating blocks (42 mm × 40 mm × 15.2 mm) hollowed out with a circular hole (8 mm diameter) which were fabricated by Automation Engineering R&M Centre (AERMC), Guangdong Academy of Sciences (Guangzhou, China), three resistance cartridge heaters (100 W, 8 mm × 40 mm (o.d. × length), Guangzhou Haoyi Thermal Electronics Factory, Guangzhou, China), three

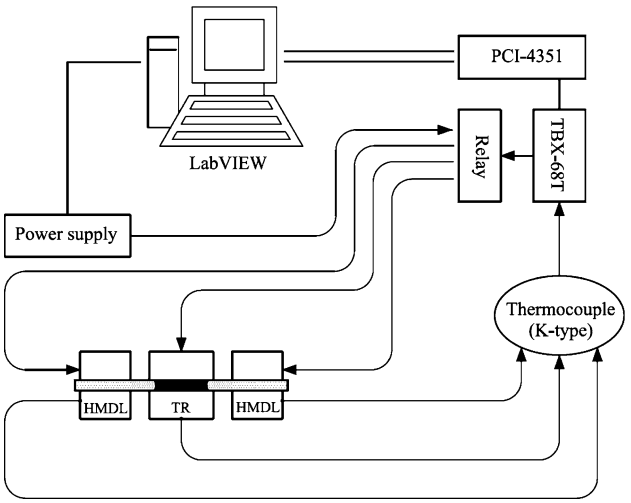

Fig. 2 Illustration of the temperature control system using the HMDL method to decrease heat-induced microfluidic evaporation loss. The microchannel with even or uneven diameter is incorporated on three constant temperature regions (two HMDL regions and one TR region)

thermocouples (K-type, 0.005 inch diameter, Omega Engineering Inc., Stamford, CT, USA), the PCI control module (PCI-4351, National Instruments Corp., Austin, TX, USA), the terminal block (TBX-68T), and the relay module. When the PCR thermocycling is performed, the copper heating block of the TR region is replaced with the thermoelectric (TE) unit (40 mm × 40 mm, output power of 30 W) that is powered with a DC power supply (Model PS-305D, Longwei Instrument Meter Co. Ltd., Hongkong, China). The control of thermal cycling or constant temperature was performed with a LabView™ (Version 8.0, National Instrument Corp., Austin, TX, USA) program through the PCI control module. A K-type thermocouple, which was inserted into the bore of the copper heater block or placed onto the upper surface of TE unit, was connected to the terminal block which, in turn, interfaced with the PCI control module. The temperature acquired with the thermocouple was used as the feedback signal for the fuzzy proportional/integral/derivative (PID) algorithm that was programmed in LabView™.

2.3 Formation of the microreservoir for evaluating the HMDL method

In order to demonstrate that the HMDL method can be used to decrease the heat-induced microfluidic evaporation loss, a series of channel microreservoirs with same length are constructed. Unless otherwise stated, the length of the TR region is 40 mm, and the length of each HMDL side is 27 mm. In between two adjacent copper blocks, an air gap of ~3 mm is used to secure thermal insulation. As a result, the total length of about 100 mm is used. When the microchannels within the TR and HMDL regions have different cross-sections, they are assembled together with the home-made miniaturized connectors. It should be noted that the channel microreservoir is placed onto the horizontal heating blocks to prevent the gravity-induced liquid flow. During experimental runs, it has been observed that the liquid of interest can steadily settle in the TR region within a long time. In addition, the ten parallel grooves of certain width and depth are formed on the surface of the copper heater. After the channel microreservoirs are embedded into these grooves, they are covered with a thin layer of transparent glass cover whose edges are in contact with a raised piece of the copper block. Such design can improve temperature uniformity inside the channel microreservoir.

2.4 Experimental procedures

After the channel microreservoir is washed and desiccated, the liquid of interest is introduced into the microchannel of the TR region via capillary force, without need of any pipetter or pump. The filled channel microreservoir with/without the HMDL sides is then laid on the desired temperature regions. When the HMDL method is used, the temperature block of the HMDL region is first heated to the desired temperature (T_{HMDL}) (for example 105°C), the temperature of the TR region (T_{TR}) is regulated according to the experimental requirements (for example 95°C). Figure 3 shows the typical curves of the T_{HMDL} and T_{TR} as a function of time. As shown in Fig. 3, the T_{HMDL} is heated to 105°C and keeps constant after about 90 s. In this work, the TR region begins to be heated after the HMDL region is heated for 120 s, and the time when the TR region begins to be heated is considered as the origin of the time scale of

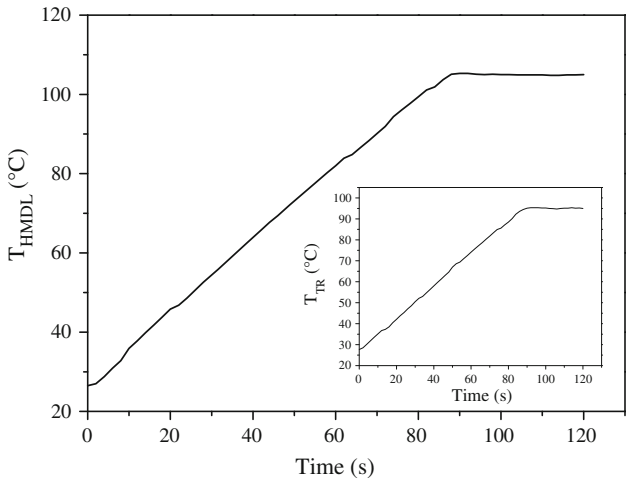

Fig. 3 A typical curve of the temperature of the HMDL region (T_{HMDL}) as a function of time. The *inset* shows a typical curve of the temperature of thermal reaction region (T_{TR}) versus time

the relative evaporation loss (time $t = 0$). In addition, data at each point is independently measured thrice. Note that the developed PID module allows the TR region to be heated to the desired T_{TR} as rapidly as possible, with an over-shoot temperature less than 1°C (Fig. 3). During the experiments, the assembled device is placed at a room environment that is air-conditioned at 25 ± 2°C. In addition, it is necessary to point out that during experimental runs, the volume of the liquid is indirectly obtained by measuring the length of liquid within the capillary channel microreservoir with the home-made measuring device, which mainly consists of an optical magnifier and a vernier caliper (Hangzhou Hanggong Tools Industry Co. Ltd., Hangzhou, China). One can freely adjust the measuring device relative to the place where the channel microreservoir is placed. The purpose of using the magnifier is to ease the observation of fluid so as to improve the precision of measurement.

2.5 Experimental materials

Taq DNA polymerase (5 unit/μl), 10 × Taq DNA polymerase buffer (500 mM KCl, 100 mM Tris–HCl (pH 8.8), 0.8% Nonider P-40), and $MgCl_2$ solution (25 mM) were purchased from Bio Basic Inc. (BBI) (Ontario, Canada). Deoxynucleotide triphosphate (dNTPs) (10 mM each of dATP, dGTP, dCTP, and dTTP in water), primers, and agarose were obtained from Shanghai Sangon Biological Engineering & Technology Services Co. Ltd. (SSBE, Shanghai, China). The sequences of forward and reverse primers were 5′-GGC CTA TAG CTC AGC TGG TTA-3′ and 5′-GCT GAG CTA AGG CCC CGT AAA-3′, respectively. With this set of primers, a DNA fragment of 135 bp is amplified. The doubly deionized H_2O (ddH_2O) and DNA markers were bought from Tiangen Biotech Co. Ltd. (Beijing, China). Bovine serum albumin (BSA) (fraction V; Cat. No. 735094) was from Roche Diagnostics GmbH (Mannheim, Germany). GoldView™ dye was purchased from SBS Genetech Co. Ltd. (Beijing, China). Glycerol (analytical reagent) was purchased from Tianjin Fuyu Fine Chemical Co., Ltd. (Tianjin, China). The *Listeria monocytogenes* (*L. monocytogenes*) CMCC54007 was obtained from Guangzhou Microbiology Institute (Guangzhou, China). The glass capillary with inner diameter (ID) 500 or 300 μm was obtained from Instrument Factory of West China University of Medical Sciences (Chengdu, China). The glass capillary tube with an ID of 50, 100, or 150 μm was provided by Yongnian Ruifeng Chromatographic Device Co., Ltd (Handan, China). Unless stated elsewhere, the liquid introduced into the TR channel for evaluation of the HMDL method consists of 1 × Taq DNA polymerase buffer, 1.5 mM $MgCl_2$ solution, 0.2 mM each dNTP, and 10% (v/v) glycerol. In this study, the purpose of use of high boiling point biocompatible glycerol is to increase the boiling point of the resulting liquid, and thus to prevent bubble formation at high temperatures.

2.6 PCR amplification and analysis

PCR in a HMDL-based open microfluidic system was demonstrated by amplifying a 135-bp fragment on the intergenic region spacer (IGS) between the 16S and 23S rRNA genes from *L. monocytogenes* genomic DNA. In parallel, control runs were performed using a Mastercycler gradient thermocycler (Eppendorf AG, Hamburg, Germany). Both the control and microfluidic PCR reactions were performed with the same reagents, which included 6.0 ng/μl DNA template, 1 × PCR buffer, 1.5 mM $MgCl_2$, 0.2 mM each dNTP, 0.4 μM each primer, 0.5 μg/μl BSA, 0.2 unit/μl Taq DNA polymerase, and 10% (v/v) glycerol. The thermocycling protocol used by the microfluidic or positive-control PCR consisted of a 94°C incubation for 2 min for initial DNA denaturation, followed by 30 or 35 PCR amplification cycles consisting of 94°C for 30 s, 55°C for 30 s, and 72°C for 1 min, and a final extension at 72°C for 2 min. PCR products were visualized and analyzed with a 1.5% agorose gel electrophoresis prestained with GoldView™ dye.

3 Results and discussion

3.1 Effect of the HMDL and TR region's temperatures (T_{HMDL} and T_{TR}) on the relative evaporation loss (V_{loss}/V_{ini})

The HMDL evaporation is a temperature-controlled method for decreasing the microfluidic evaporation loss. Therefore, the effect of T_{HMDL} on the evaporation loss is first evaluated. Figure 4a shows the relative evaporation loss (V_{loss}/V_{ini}) versus time for a variety of HMDL region's temperatures for a set value of $T_{TR} = 95$°C and uniform channel diameter of $d_{HMDL} = 300$ μm and $d_{TR} = 300$ μm, representative of a typical medium-scaled reservoir constructed from glass capillary in this study. In addition, the T_{TR} of 95°C is chosen because this temperature is not only the denaturation temperature of the used widely PCR-based DNA amplification technique, but also the temperature of cell thermal lysis that is an alternative method for disrupting cell walls or membranes. As shown in Fig. 4a, a decrease in V_{loss}/V_{ini} is seen with increasing T_{HMDL}. For example, when T_{HMDL} is 55°C, the evaporation loss (V_{loss}) in the tested channel within 60 min is approximately 33% of the initial volume of liquid (V_{ini}). For the case of $T_{HMDL} = 85$°C, there is a decrease in V_{loss}/V_{ini} during the same duration by 42% to reach ~19%. However, further increasing T_{HMDL} to

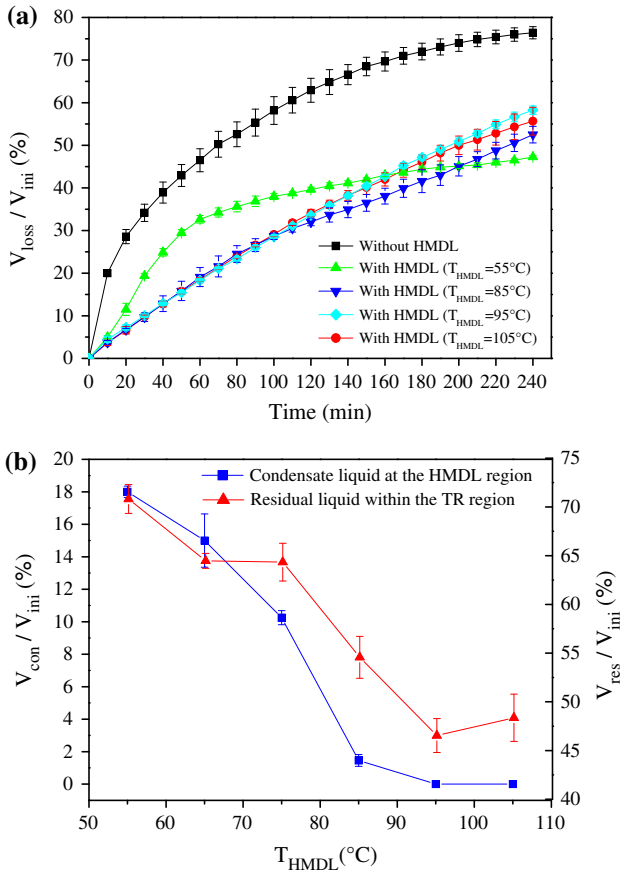

Fig. 4 **a** Effect of T_{HMDL} on the relative evaporation loss V_{loss}/V_{ini}. **b** The relative condensate liquid volume V_{con}/V_{ini} within the HMDL region and the relative residual liquid volume V_{res}/V_{ini} within the TR region as a function of temperature of the HMDL region within 240 min. $d_{HMDL} = d_{TR} = 300$ μm, $T_{TR} = 95$°C

95 or 105°C can not obviously decrease the V_{loss}/V_{ini}. In order to demonstrate the usefulness of the HMDL method, V_{loss}/V_{ini} without HMDL versus time under other same conditions is also included in Fig. 4a. It is clearly seen from Fig. 4a that the difference in relative evaporation losses between with and without HMDL is quite dramatic. The V_{loss}/V_{ini} without HMDL within 60 min is high up to 47%, which is about twice of that with HMDL at $T_{HMDL} = 85$°C. This evaporation loss is unacceptable for many microfluidic applications where the analyte(s) must be maintained within a certain concentration range.

Experimentally observed V_{loss}/V_{ini} with HMDL at $T_{HMDL} = 85$, 95, or 105°C seems to be linearly increased within the time range of 0–240 min. That is, the evaporation rate is nearly invariable. However, V_{loss}/V_{ini} without HMDL shows a non-linear and exponentially increased trend. The evaporation rate gradually reduces and finally tends to be "zero". Such experimental results can be attributed to the following reasons: (1) for evaporation without HMDL, the diffusion length gradually increases as the menisci at both ends of a channel reservoir recedes (the initial diffusion length without HMDL is close to be zero). In general, the increase in the average distance needed for diffusion will result in the decreased evaporation rate (Lynn et al. 2009). However, for the case of evaporation with HMDL, the initial diffusion length at each end of the TR region is about 30 mm. During evaporation, the increased diffusion length is far less than this initial diffusion length, and therefore the evaporation rate shows near-linear. (2) For the zero diffusion length without HMDL, the liquid of interest will be exposed to a ventilated environment that increases evaporation rates (Berthier et al. 2008a). In most cases, the absolutely windless laboratory environment is hard to obtain. However, for the HMDL region with a diffusion length of about 30 mm at each end, this ventilation-induced effect on evaporation loss of liquid is negligible.

Here, it should be accentuated that the curve with HMDL at 55°C developed exponentially as without HMDL. The reasons for this phenomenon can be explained as follows: when T_{HMDL} becomes 55°C, the vapor from the TR region ($T_{TR} = 95$°C) gradually condenses, continuously decreasing the concentration of vapor within the diffusion channel. As a result, at the early stage the evaporation rate within the TR channel with HMDL is still high (Fig. 4a). However, the amount of the condensate liquid increases with time, and the liquid 'plug' forms at the place adjacent to the TR region after about 60 min. It has been found that when the liquid plug forms, the evaporation rate within the TR channel begins to decrease. This is most likely because under the similar conditions, the evaporation rate of liquid at 55°C is much lower than that at 95°C. In addition, the formed plug of liquid seems acts as the "valve" to decrease the diffusion of vapor within the TR region. However, for the case of HMDL at 85°C, the condensed water in HMDL section greatly decreases. Even at the early stage (for example within 120 min), it is hard to observe the formation of the condensed water. Within ~240 min, its volume of the condensed water is only 1% of the initial liquid volume. As a result, during the experiments, it cannot form the liquid plug. This result can be attributed to the following reason: when the air gap of ~3 mm is used between two adjacent copper heating blocks, the microchannel between them suffers from a gradually decreased temperature gradient from the TR region (95°C) to the HMDL region (85°C). While the vapor evaporated from the TR region diffuses through this region, its temperature gradually decreases, but its saturation temperature is still very close to the temperature of channel innersurface within this region. Therefore, the phenomenon that the condensed water in the HMDL region affects the evaporation of liquid within the TR region is not apparent for the case of HMDL at 85°C.

As stated previously, the HMDL method developed here makes full use of the liquid condensated at the DL region and the long-armed DL evaporation to decrease heat-induced microfluidic evaporation loss. Figure 4b displays the relative condensate liquid volume V_{con}/V_{ini} in the HMDL region and the relative residual liquid volume V_{res}/V_{ini} in the TR region as a function of T_{HMDL} within 240 min. It has been shown that V_{con}/V_{ini} or V_{res}/V_{ini} gradually reduces with increasing T_{HMDL}. For example, at $T_{HMDL} = 55°C$, the volumes of condensate liquid within the HMDL regions and residual liquid within the TR region are $\sim$18 and 71% of the original liquid volume, respectively. For the case of $T_{HMDL} = 85°C$, the volumes of corresponding liquid within each region decrease to $\sim$1 and $\sim$54%, respectively. The small amount of condensate liquid still remains within the HMDL regions. When T_{HMDL} is further increased to 95 or 105°C, condensation does not take place. In the experimental results described below, 105°C is chosen for T_{HMDL} in each case, similar to the working manner of the heated lid in the conventional PCR machines.

In addition to T_{HMDL}, T_{TR} also affects V_{loss}/V_{ini} or evaporation rate. It is of great importance to evaluate the effects of the T_{TR} since different T_{TR} used within the TR region will associate with different potential applications of the HMDL method, such as some isothermal amplification reactions that have been well used to produce large numbers of amplification products from small biological samples. In general, different isothermal reactions require different constant temperatures such as MDA (30°C), RCA (30–37°C), NASBA (41°C), LAMP (60–65°C), reverse transcription reaction (42–50°C), enzyme digestion reaction (37°C), and padlock ligation reaction (50°C). As is known, the driving force for liquid evaporation is the difference between the interfacial vapor pressure p_v and the ambient vapor pressure p_0, and p_v is strongly associated with the interfacial temperature T_i. For the experiments performed in this work, all liquid of interest is ensured to be situated in the desired TR region. Therefore, the relative evaporation loss is dependent on the T_{TR}. Figure 5 shows the dependence of V_{loss}/V_{ini} without/with HMDL on T_{TR}. The comparison between Fig. 5a and b further shows that the HMDL approach has an acute effect in reducing the microfluidic evaporation loss. Furthermore, for the two cases presented, V_{loss}/V_{ini} reduces with decrease of T_{TR}. For example, when the HMDL regions are used, V_{loss}/V_{ini} at $T_{TR} = 95$, 72, 65, 55, and 45°C within 60 min is approximately 19, 6, 5, 4, 3%, respectively. As much as within 120 min, V_{loss}/V_{ini} at corresponding T_{TR} is about 34, 12, 10, 8, and 5%, respectively, showing a slight increase in V_{loss}/V_{ini}. Such results have shown that the HMDL technique in this study can be used for the above-mentioned biological and chemical applications where the isothermal reactions are required.

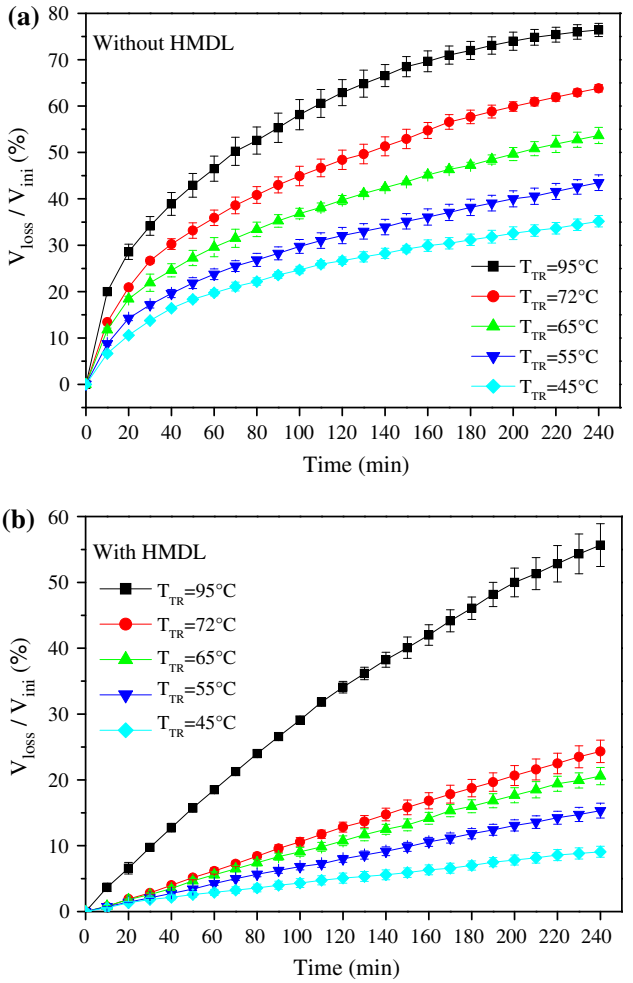

Fig. 5 Effect of T_{TR} on the relative evaporation loss. **a** Without the HMDL region ($d_{TR} = 300$ μm). **b** With the HMDL region ($d_{HMDL} = d_{TR} = 300$ μm, $T_{HMDL} = 105°C$)

3.2 Effect of HMDL and TR's channel geometries on the relative evaporation loss (V_{loss}/V_{ini})

Experimental observed evaporation rates of liquids contained in certain reservoirs have been shown to be strongly associated with the geometry of the reservoir. For example, Lynn et al. have shown that the evaporation rate is higher for an expanding reservoir than a contracting reservoir for a given volume of liquid (Lynn et al. 2009). Wang et al. (2008) also showed that the cross-sectional area of the channel affected the V_{loss}/V_{ini} ratio. In this work, a simple reservoir design consisting of a straight channel with uniform cross-section area is first used to evaluate the effects of different cross-section areas on the V_{loss}/V_{ini} and evaporation rate (Fig. 6). For the two cases with/without HMDL, within the same duration of time both V_{loss}/V_{ini} and average evaporation rate decrease with reducing diameters of the channel. For $d_{HMDL} = d_{TR} = 500$, 300, and 100 μm, the V_{loss}/V_{ini} with HMDL within 60 min are

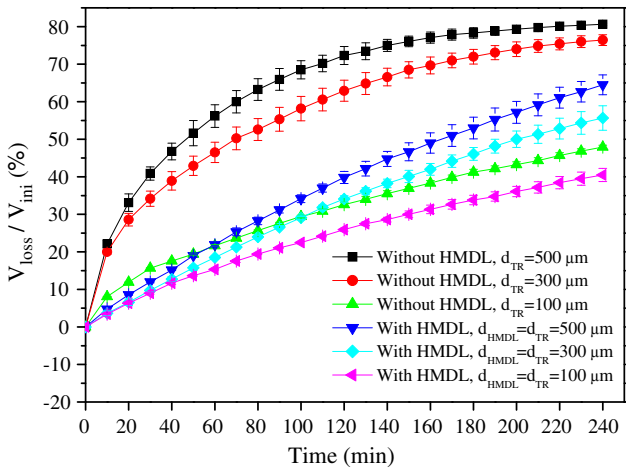

Fig. 6 The relative evaporation loss with/without the HMDL region V_{loss}/V_{ini} as a function of time within the uniform channel reactors with different diameters. $T_{HMDL} = 105°C$, $T_{TR} = 95°C$

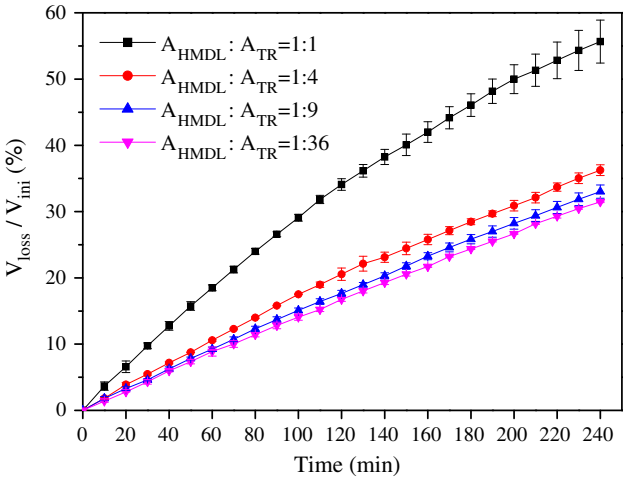

Fig. 7 Effect of the cross-sectional area of the HMDL channel (A_{HMDL}) on the relative evaporation loss. In all cases, the cross-sectional area of the thermal reaction region (A_{TR}) is constant ($d_{TR} = 300$ μm), the d_{HMDL} within the HMDL region is 50, 100, 150, and 300 μm, respectively. $T_{HMDL} = 105°C$, $T_{TR} = 95°C$

approximately 22, 18, and 15%, respectively. Under other same conditions, the V_{loss}/V_{ini} without HMDL are high up to approximately 56, 46, and 21%, respectively. The evaporation rates are reduced in channels of small diameter due to the decrease in the available interfacial area for diffusion area. It should be noted that the evaporation loss without HMDL changes more rapidly than that with HMDL. For example, V_{loss}/V_{ini} without HMDL within 60 min sharply reduces from 47% at $d_{TR} = 300$ μm to 22% at $d_{TR} = 100$ μm. Under other same conditions, however, the relative evaporation loss with HMDL for $d_{TR} = 100$ μm ($V_{loss}/V_{ini} = 15\%$) is only slightly lower than the case for $d_{TR} = 300$ μm ($V_{loss}/V_{ini} = 18\%$). These results show that within straight small channels with uniform cross-section area, V_{loss}/V_{ini} with HMDL is lower than that without HMDL, but has little dependence on the diameter of small channel. In fact, although the absolute value of evaporate loss is very small when the thin channel is used, V_{loss}/V_{ini} is still large due to the small initial volume of liquid.

Different from the uniform channels, the straight channels with varying cross-sectional area would have the ability to further decrease V_{loss}/V_{ini}. During the experiments, the straight channel is divided into three regions: one TR region with the cross-sectional area A_{TR} and two HMDL regions on either end of the TR region with the cross-sectional area A_{HMDL}. Figure 7 illustrates the effect of the A_{HMDL} on V_{loss}/V_{ini}. It needs to be noted that in all cases, the d_{TR} within the TR region keeps constant ($d_{TR} = 300$ μm), but the d_{HMDL} in the HMDL region is changeable ($d_{HMDL} = 50$, 100, 150, and 300 μm). The results in Fig. 7 shows that the smaller the value of A_{HMDL}:A_{TR} is, the less the V_{loss}/V_{ini} will be, implying that the narrow HMDL channels with large TR channels are preferred. For example, when the A_{HMDL}:A_{TR} ratio changes from 1:1 to 1:4, the V_{loss}/V_{ini} within 60 min decreases from 19 to 10%. However, to further decrease this ratio, only results in a litter decrease in V_{loss}/V_{ini}. For two cases of both A_{HMDL}:$A_{TR} = 1:9$ and 1:36, the V_{loss}/V_{ini} within 60 min keeps approximately 9%. As was demonstrated before (Wang et al. 2008), the evaporation rates may increase in narrow channels due to the increased extent of liquid film wetting on the channel wall. However, it has been clearly shown in Fig. 7 that this functional relationship does not hold true for the HMDL method in this study. One possible reason for this phenomenon is that the liquid film is hard to form on the channel wall since the HMDL channel is maintained in the high temperature environment (up to 105°C). Note that when T_{HMDL} keeps low (for example 85 or 55°C), the vapor evaporated from the TR region ($T_{TR} = 95°C$) condenses at the HMDL region and the condensate wets the surface of HMDL channel and forms a liquid film on the surface. Moreover, this wetting would be extended by narrowing the d_{HMDL} in the HMDL region, and thus the film evaporation rate may increase. However, shrinking the diameter of HMDL section will greatly decrease the diffusion rate of vapor within the tested channel. In addition, under other same conditions, the evaporation rate of liquid at $T_{HMDL} = 85$ or 55°C is lower than that at $T_{TR} = 95°C$. As a result, when the d_{HMDL} is decreased for the case of low T_{HMDL}, the net V_{loss}/V_{ini} should be decreased. However, decreasing the d_{HMDL} within the HMDL region has no or little effect on the wetting within the TR section since the d_{TR} at the TR region keeps constant.

In addition to the effects of the A_{HMDL} on the V_{loss}/V_{ini}, the A_{TR} and geometry of the TR channel have also an active effect on the V_{loss}/V_{ini}. Figure 8a illustrates the schematic of a straight channel (d_{TR} = 300 μm, d_{HMDL} = 200 μm) and U-shape channel (d_{TR} = d_{HMDL} = 200 μm), giving a same initial volume of 3 μl for the TR channel. Figure 8b shows the V_{loss}/V_{ini} as a function of time in two cases of Fig. 8a. For a given volume of liquid, the V_{loss}/V_{ini} and evaporation rate within the thin TR channel are much lower than those within the thick TR channel due to the decrease in the available area for diffusion area as d_{TR} decreases. For example, the V_{loss}/V_{ini} within 60 min decreases from 14% for d_{TR} = 300 μm to 5% for d_{TR} = 200 μm, and the average evaporation rate has also a similar dependence on d_{TR}. This result shows that to perform the TR with same volume of liquid and HMDL channel, thin TR channels are preferred. Moreover, in order to decrease the footprint of device, the U-shaped or serpentine TR channels should be used.

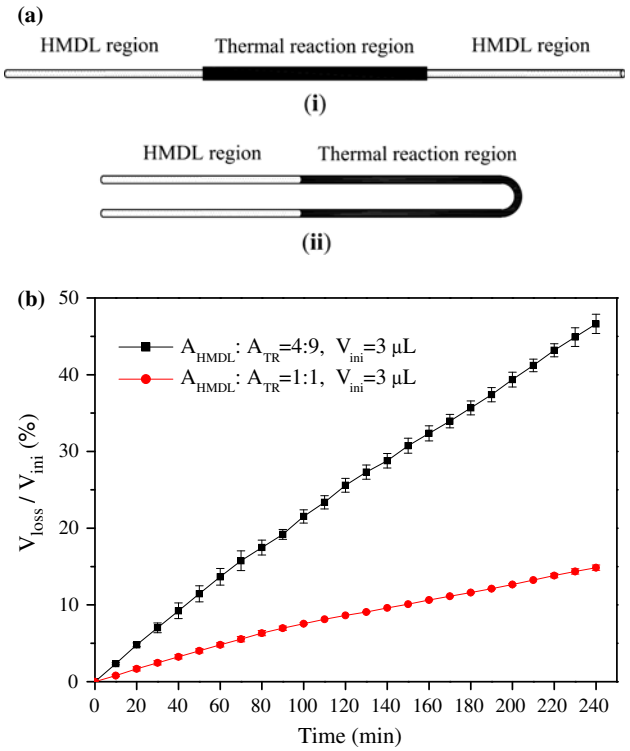

Fig. 8 Effect of the cross-sectional area (A_{TR}) and geometry of the TR channel on the relative evaporation loss. **a** Schematic of the straight channel (**i**) (d_{TR} = 300 μm, d_{HMDL} = 200 μm) and U-shape channel, (**ii**) (d_{TR} = d_{HMDL} = 200 μm), giving a same initial volume of 3 μl for the thermal reaction region. **b** The relative evaporative loss V_{loss}/V_{ini} as a function of time in two cases of (**a**). T_{HMDL} = 105°C, T_{TR} = 95°C

3.3 Applications of HMDL-based open microfluidic systems to PCR thermocycling systems

One of our goals in this study is to develop an open microfluidic system for PCR thermocycling so as to circumvent the problems associated with solid/liquid lids or microvalves that are often used to seal the TR microreservoirs to reduce the evaporation loss. The aforementioned experiments on the V_{loss}/V_{ini} as a function of time (Figs. 4, 5, 6, 7, 8) are all performed at the constant T_{TR}, with the result that lower V_{loss}/V_{ini} can be obtained at these temperatures within a relative long time (for example 60 min). By considering and comparing the results in Figs. 5, 6, and 7, it is reasonable to think that the HMDL method can be used to construct an open microfluidic systems for PCR thermocycling. Figure 9a displays the thermocycling curve of the straight channel-based TR microreservoir (d_{TR} = 300 μm, d_{HMDL} = 300 or 100 μm) within the TR region (only 16 cycles were shown). The thermal cycle protocol started with a 2-min 94°C initial denaturation step followed by 40 cycles of 0.5 min at 94°C, 0.5 min at 55°C, and 1 min at 72°C, with a final extension of 2 min at 72°C, giving a total reaction time of about 154 min. The V_{loss}/V_{ini} as a function of the number of PCR cycles is shown in Fig. 9b, where the A_{HMDL}:A_{TR} is 1:1 (d_{HMDL} = d_{TR} = 300 μm) or 1:9 (d_{HMDL} = 100 μm, d_{TR} = 300 μm). For two cases, the V_{loss}/V_{ini} seems to linearly increase with increase of number of PCR cycles. After 35 cycles, the V_{loss}/V_{ini} is ~19% for A_{HMDL}:A_{TR} = 1:1 and ~10% for A_{HMDL}:A_{TR} = 1:9. In the PCR microfluidic devices reported before, the effect of the sample evaporation loss on PCR amplification has been investigated by some searchers. For example, Prakash et al. (2006) have observed that samples that lost more than about 50% of their volume during the PCR stage were generally unsuccessfully amplified. In this context, the PCR may only be successful if it is started with a sufficiently large number of DNA molecules, so as to obtain a detectable amount of PCR product after about 20 cycles. After 35 thermal cycles, the PDMS chip, where the volume of liquid lost was only about 0.4 μl, i.e., about a 23% fluid loss, could give a reliable PCR result, using samples with either a large or small number of template molecules (Prakash et al. 2006). Note that Prakash et al. did not compensate for the changes in the concentration of the salts and other possible PCR inhibitors by the 23% loss of fluid. Therefore, the HMDL-based open microfluidic system developed here is suitable for PCR thermocycling.

To demonstrate that PCR can be achieved on the HMDL-based open microfluidic system, three-parallel amplification of a 135-bp gene fragment from *L. monocytogenes* genomic DNA was performed on the current device using the straight channel-based TR microreservoir (d_{TR}=300 μm,

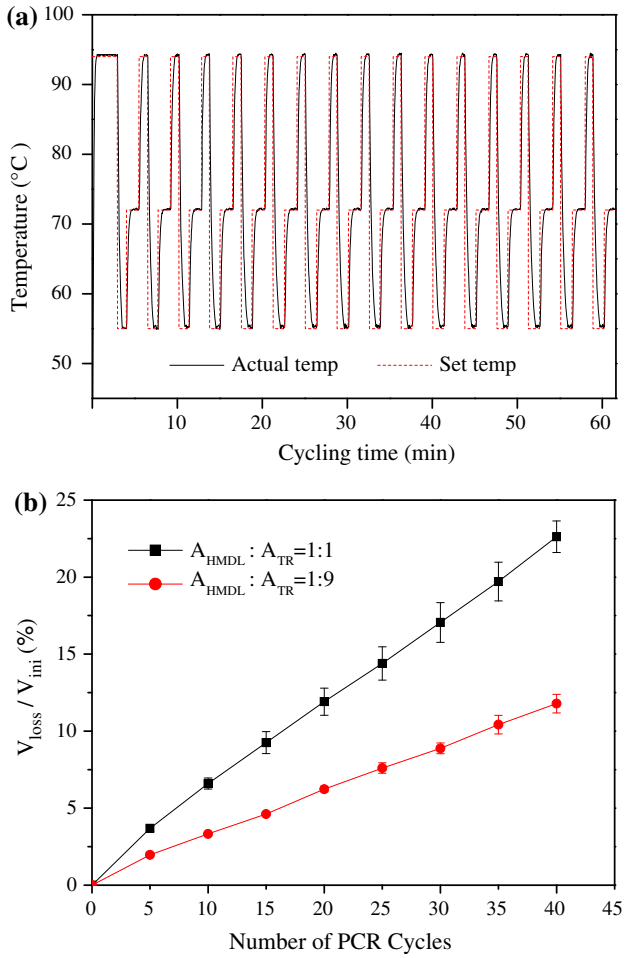

Fig. 9 **a** Temperature cycling curve of the straight channel-based TR microreservoir (d_{TR} = 300 μm, d_{HMDL} = 300 or 100 μm) (only 16 temperature cycles were shown). The thermocycling profile consisted of 94°C for 2 min for the initial denaturation, 40 cycles of 94°C for 0.5 min, 55°C for 0.5 min, and 72°C for 1 min, followed by 2 min at 72°C for a final extension, which gave a total reaction time of about 154 min. **b** The relative evaporative loss V_{loss}/V_{ini} as a function of the number of PCR cycles when the A_{HMDL}:A_{TR} is 1:1 (d_{HMDL} = d_{TR} = 300 μm) or 1:9 (d_{HMDL} = 100 μm, d_{TR} = 300 μm). T_{HMDL} = 105°C

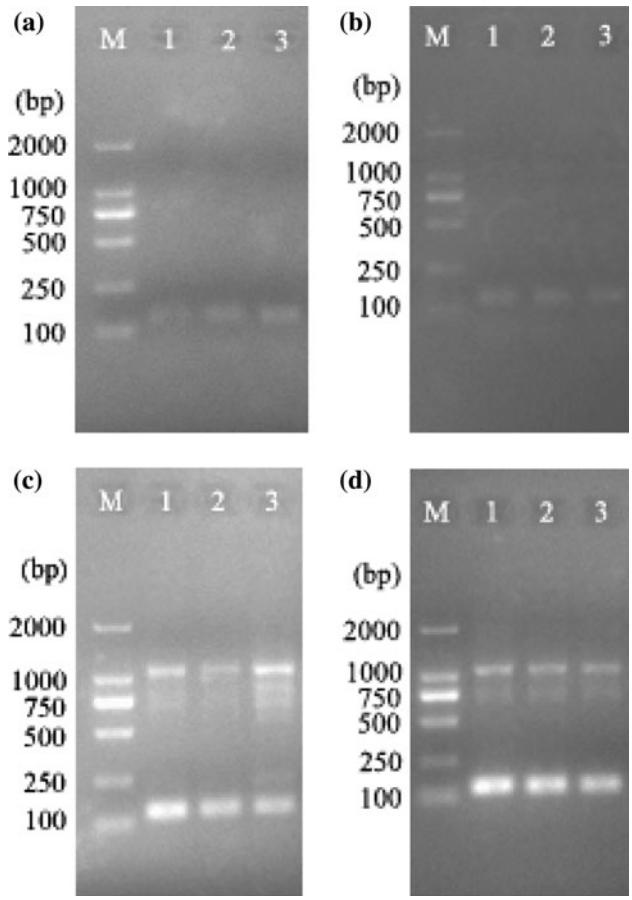

Fig. 10 Electrophoretic assessment of PCR products obtained using the HMDL-based PCR microfluidic system and the commercial thermocycler. **a** and **b** were the PCR products after 30 thermal cycles using the HMDL-based microfluidic system and the commercial PCR system. **c** and **d** were the 35-cycle PCR products performed in the HMDL-based microfluidic system and the commercial PCR system. *Lane M*, DNA markers, *Lanes 1–3*, three-parallel PCR reactions under the same reaction conditions. And, the used thermocycling parameters are demonstrated in Fig. 9 (d_{TR} = 300 μm, d_{HMDL} = 100 μm)

d_{HMDL}=100 μm) and the thermocycling parameters described in Fig. 9. Figure 10a, b shows the PCR products collected from the open microfluidic system and the commercial thermocycler after 30 thermal cycles. It has shown that open microfluidic PCR exhibits similar amplification efficiency to the positive control in the commercial PCR thermocycler, and that no byproduct bands have been detected from two reaction systems. After 30 thermal cycles, the V_{loss}/V_{ini} is approximately 9% for the open reaction system. It is necessary to note that during the open system-based PCR runs, the same reagent components were used as those in the commercial apparatus, and the reaction protocol was not optimized, indicating the robustness of the HMDL-based open PCR system. However, some nonspecific side-products were found when 35 thermal cycles were used in the current open reaction system, as shown in lanes 1–3 of Fig. 10c, where the V_{loss}/V_{ini} is about 10.5%. To test whether the production of the unspecific byproducts is due to the increased evaporation loss resulted from the increase of PCR cycles, the 35-cycle positive-control PCR was also carried out in the commercial thermocycler under the similar reaction conditions (Fig. 10d). The results showed that the nonspecific PCR products appeared in each of three-parallel positive controls. Therefore, the unspecific byproducts detected after 35 cycles within the HMDL-based open PCR system are not due to the increased evaporation loss, but due to the PCR chemistry itself and/or the thermal cycling protocol. By using the optimized PCR components and thermocycling parameters, the increase of the number of cycles maybe will not result in the unspecific byproducts.

The current thermal cycling for the HMDL-based open PCR microfluidic system is performed in a commercial Peltier device controlled by the fuzzy PID strategy. The thermocycling device is not optimized and efficient temperature transitions of only ~1.0°C/s are achieved. Most of the cycling time is spent on cooling and heating during the reaction process. As a result, a 40-cycle PCR thermocycling needs to be completed within 154 min, and the V_{loss}/V_{ini} is ~23% (A_{HMDL}:A_{TR} = 1:1) and ~12% (A_{HMDL}:A_{TR} = 1:9) during this duration. In order to decrease V_{loss}/V_{ini} during the thermal cycling, the heating/cooling rates should be increased. Although the high thermal mass of the Peltier device weakens the thermal response of the entire PCR microdevice, ~5°C/s heating rates can still be acquired (Prakash et al. 2006). Alternatively, the microelectromechanical systems (MEMS)-based film heaters have a smaller thermal mass, and thus allow faster thermal response and heating rates high up to 10°C/s. To date, the fastest heating rate (175°C/s) and cooling rate (125°C/s) have been obtained using this method, where 40 PCR cycles can be accomplished in <6 min (Neuzil et al. 2006). Currently, we are examining improved designs of thermal cycling to increase the heating/cooling rates to decrease the cycling time. The improved design provides powerful DNA amplification by using the HMDL-based open microfluidic PCR system.

3.4 Comparison of different methods to decrease/prevent liquid evaporation loss within microfluidic systems

In previous studies, various methods of reducing/preventing liquid evaporation loss within close or open microfluidic systems have been well developed. Several typical results are compared and listed in Table 1. In general, solid covers can be used to seal the liquid sample to form a close microfluidic system, where liquid sample evaporation is greatly reduced and no appreciable evaporation loss can be observed over a long period (Cho et al. 2006; Moerman et al. 2005). The principle of this approach is to resist the internal pressure generated during thermal reactions. It is known that the evaporation rate reduces with the increase of gas pressure around a liquid. Cheng et al. (2005) have recently developed an improved solid cover approach to decrease sample evaporation within the oscillating-flow PCR chip. In their approach, a single opening serves for both sample loading and syringe pump port. When the sample plug is pumped to high-temperature zones, the internal pressure increases by six times and thus the sample evaporation is greatly reduced. It has shown that ~70% of the sample remains as a unified plug following 30 temperature cycles. As stated above, however, the solid cover approach will increase the complexity of fabrication and

Table 1 Comparison of methods of decreasing/preventing evaporation loss within microfluidic systems

Method	Field of application	Heat condition	Volume of liquid	Evaporation loss	Reference
Heat-mediated diffusion-limited (HMDL)	Steady flow PCR	60 min at 95°C	~3 µl	~5%	This work
		35 cycles (30 s at 94°C, 30 s at 55°C, 60 s at 72°C); heating/cooling rate: ~1.0/~1.0 (°C/s)	~3 µl	~10%	
Diffusion-limited evaporation with thermal isolation and vapor replenishment	Steady flow PCR	35 cycles (5 s at 94°C, 10 s at 55°C, 20 s at 72°C); heating/cooling rate: ~4.5/~4.5 (°C/s)		~1%	Wang et al. 2008
Mineral oil cover	Steady flow PCR	35 cycles; heating/cooling rate: 10/5 (°C/s)	200 nl	10%	Guttenberg et al. 2005
Sealing the inlet/outlet holes using the tape	Steady flow PCR	40 cycles (1 s at 92°C, 15 s at 62°C)	1 µl	No appreciable evaporation	Cho et al. 2006
Vapour barrier	Steady flow PCR	35 cycles (60 s at 94°C, 60 s at 55°C, 60 s at 72°C); heating/cooling rate: ~ 4.5/~ 4.5 (°C/s)	~1.75 µl	~23%	Prakash et al. 2006
Pressurizing the sample during heating	Dynamic flow PCR	30 cycles shuttled along a radial temperature gradient	6 µl	~30%	Cheng et al. 2005
Solid coverslip	Enzyme reaction		8 nl	No appreciable evaporation for minutes up to hours	Moerman et al. 2005
Volatile liquid cover	Tryptic digest	90 min at 37°C	15 nl	No appreciable evaporation	Litborn and Roeraade 2000
		>3 min at 95°C		Very small loss	

fluidic handling. Apart from regular solid lids, a liquid cover in the form of a high-boiling mineral oil has been employed for PCR systems. By using the mineral oil cover, the loss of water by evaporation from the droplet after 35 PCR cycles was about 10% (Guttenberg et al. 2005). Encapsulation of the PCR solution against evaporation can be reached much simpler than with solid cover or microvalves in a microfluidic channel system (Guttenberg et al. 2005). However, a mineral oil lid is difficult to remove from very small fluid volumes. In addition, it contaminates and obstructs the inlet of micro-pipettes during withdrawal of an aliquot of sample, and disturbs subsequent analysis (Litborn and Roeraade 2000).

As demonstrated above, simple microfluidic devices are usually open or unsealed systems to ease the introduction and/or withdrawal of an aliquot of sample, without any disturbance of subsequence analysis. In the literature, there is a report of microfluidic valveless device for open PCR thermal cycling based on diffusion-limited evaporation (Wang et al. 2008). In this work, three valveless strategies have been developed to reduce the sample evaporative loss in a microfluidic device during thermal reactions using the principle of diffusion-limited evaporation, including use of long narrow diffusion channels, decreasing the interfacial temperature using thermal isolation, and reducing the vapor concentration gradient by replenishing water vapor in the diffusion channels. Although the proposed approaches can limit the evaporation loss to approximately 1% of the reaction content, both thermal isolation and vapor replenishment techniques are complicated in design, and high in the chip fabrication and operation cost. When compared to the work of Wang et al. (2008), the HMDL method proposed in this article does not require complicated thermal isolation to reduce the interfacial temperature, or external pure water to be heated synchronously with the reaction chamber to increase the vapor concentration in the diffusion channel and therefore decrease the concentration gradient. Using the HMDL method, the evaporation loss is only 15% within a comparatively long time (i.e., 240 min) in the case of $T_{TR} = 95°C$. In addition, the HMDL method only requires the fluid channel(s) and temperature controls. Therefore, the resulting microsystem is simple, and allows us to carry out a very large number of parallel-operated reactions.

4 Conclusions

In this work, we have developed the HMDL strategy to reduce the sample evaporation loss during microfluidic thermal reactions, without need of liquid/solid lid, microvalve, or sacrificial water. The principle of the method is simple and novel, and it makes the most of the evaporated reaction liquid to increase the vapor concentration in the diffusion channel. It is therefore a self-contained vapor replenishment methodology to reduce heat-induced evaporation loss. The heated microchannels on both ends of the TR region provide long narrow diffusion paths to decrease the evaporation rate. It has been shown experimentally that the V_{loss}/V_{ini} within a relatively long time (for example 60 min) is low up to 5%. This is for the first time reported within open PCR microfluidic devices, without need of any thermal isolation, vapor replenishment, solid/oil lid, or microvalves. Although PCR has been taken as an example to demonstrate the usefulness of the HMDL-based open microfluidic devices, the novel methodology can also be applied in microfluidic devices for other biological and chemical reactions. Moreover, the developed HMDL method can be readily applied onto more advanced chip-based devices where the film heater and sensor are integrated to measure and control the temperatures of HMDL and TR regions.

Acknowledgments This research is supported by the National Natural Science Foundation of China (30700155), the Key Program of NSFC-Guangdong Joint Funds of China (U0931005), the Program for Changjiang Scholars and Innovative Research Team in University (IRT0829) and the National High Technology Research and Development Program of China (863 Program) (2007AA10Z204).

References

Berthier E, Warrick J, Yu H, Beebe DJ (2008a) Managing evaporation for more robust microscale assays—Part 1. Volume loss in high throughput assays. Lab Chip 8:852–859

Berthier E, Warrick J, Yu H, Beebe DJ (2008b) Managing evaporation for more robust microscale assays—Part 2. Characterization of convection and diffusion for cell biology. Lab Chip 8:860–864

Blazej RG, Kumaresan P, Mathies RA (2006) Microfabricated bioprocessor for integrated nanoliter-scale Sanger DNA sequencing. Proc Natl Acad Sci USA 103:7240–7245

Bratten CDT, Cobbold PH, Cooper JM (1997) Micromachining sensors for electrochemical measurement in subnanoliter volumes. Anal Chem 69:253–258

Cheng JY, Hsieh CJ, Chuang YC, Hsieh JR (2005) Performing microchannel temperature cycling reactions using reciprocating reagent shuttling along a radial temperature gradient. Analyst 130:931–940

Cho YK, Kim J, Lee Y, Kim YA, Namkoong K, Lim H, Oh KW, Kim S, Han J, Park C, Pak YE, Ki CS, Choi JR, Myeong HK, Ko C (2006) Clinical evaluation of micro-scale chip-based PCR system for rapid detection of hepatitis B virus. Biosens Bioelectron 21:2161–2169

Dimov IK, Garcia-Cordero JL, O'Grady J, Poulsen CR, Viguier C, Kent L, Daly P, Lincoln B, Maher M, O'Kennedy R, Smith TJ, Ricco AJ, Lee LP (2008) Integrated microfluidic tmRNA purification and real-time NASBA device for molecular diagnostics. Lab Chip 8:2071–2078

Easley CJ, Karlinsey JM, Bienvenue JM, Legendre LA, Roper MG, Feldman SH, Hughes MA, Hewlett EL, Merkel TJ, Ferrance JP, Landers JP (2006) A fully integrated microfluidic genetic analysis

system with sample-in–answer-out capability. Proc Natl Acad Sci USA 103:19272–19277

Effenhauser CS, Harttig H, Krämer P (2002) An evaporation-based disposable micropump concept for continuous monitoring applications. Biomed Microdevices 4:27–32

Eijkel JCT, van den Berg A (2005) Water in micro- and nanofluidics systems described using the water potential. Lab Chip 5:1202–1209

Ericsson O, Jarvius J, Schallmeiner E, Howell M, Nong RY, Reuter H, Hahn M, Stenberg J, Nilsson M, Landegren U (2008) A dual-tag microarray platform for high-performance nucleic acid and protein analyses. Nucleic Acids Res 36:e45

Goedecke N, Eijkel J, Manz A (2002) Evaporation driven pumping for chromatography application. Lab Chip 2:219–223

Gulliksen A, Solli L, Karlsen F, Rogne H, Hovig E, Nordstrøm T, Sirevåg R (2004) Real-time nucleic acid sequence-based amplification in nanoliter volumes. Anal Chem 76:9–14

Guttenberg Z, Müller H, Habermüller H, Geisbauer A, Pipper J, Felbel J, Kielpinski M, Scriba J, Wixforth A (2005) Planar chip device for PCR and hybridization with surface acoustic wave pump. Lab Chip 5:308–317

Hashimoto M, Barany F, Soper SA (2006) Polymerase chain reaction/ligase detection reaction/hybridization assays using flow-through microfluidic devices for the detection of low-abundant DNA point mutations. Biosens Bioelectron 21:1915–1923

Heuck F, Hug T, Akiyama T, Frederix PLTM, Engel A, Meister A, Heinzelmann H, de Rooij NF, Staufer U (2008) Evaporation based micro pump integrated into a scanning force microscope probe. Microelectron Eng 85:1302–1305

Hutchison CA 3rd, Smith HO, Pfannkoch C, Venter JC (2005) Cell-free cloning using Φ29 DNA polymerase. Proc Natl Acad Sci USA 102:17332–17336

Kopp MU, de Mello AJ, Manz A (1998) Chemical amplification: continuous-flow PCR on a chip. Science 280:1046–1048

Lam L, Sakakihara S, Ishizuka K, Takeuchi S, Arata HF, Fujita H, Noji H (2008) Loop-mediated isothermal amplification of a single DNA molecule in polyacrylamide gel-based microchamber. Biomed Microdevices 10:539–546

Legendre LA, Bienvenue JM, Roper MG, Ferrance JP, Landers JP (2006) A simple, valveless microfluidic sample preparation device for extraction and amplification of DNA from nanoliter-volume samples. Anal Chem 78:1444–1451

Litborn E, Roeraade J (2000) Liquid lid for biochemical reactions in chip-based nanovials. J Chromatogr B 745:137–147

Litborn E, Emmer A, Roeraade J (1999) Chip-based nanovials for tryptic digest and capillary electrophoresis. Anal Chim Acta 401:11–19

Litborn E, Emmer A, Roeraade J (2000) Parallel reactions in open chip-based nanovials with continuous compensation for solvent evaporation. Electrophoresis 21:91–99

Lynn NS, Henry CS, Dandy DS (2009) Evaporation from microreservoirs. Lab Chip 9:1780–1788

Marcy Y, Ishoey T, Lasken RS, Stockwell TB, Walenz BP, Halpern AL, Beeson KY, Goldberg SMD, Quake SR (2007) Nanoliter reactors improve multiple displacement amplification of genomes from single cells. PLoS Genet 3:e155

Matsubara Y, Kerman K, Kobayashi M, Yamanura S, Morita Y, Tamiya E (2005) Microchamber array based DNA quantification and specific sequence detection from a single copy via PCR in nanoliter volumes. Biosens Bioelectron 20:1482–1490

Michikawa Y, Sugahara K, Suga T, Ohtsuka Y, Ishikawa K, Ishikawa A, Shiomi N, Shiomi T, Iwakawa M, Imai T (2008) In-gel multiple displacement amplification of long DNA fragments diluted to the single molecule level. Anal Biochem 383:151–158

Minarik M, Klepárnik K, Gilár M, Foret F, Miller AW, Sosic Z, Karger BL (2002) Design of a fraction collector for capillary array electrophoresis. Electrophoresis 23:35–42

Moerman R, Knoll J, Apetrei C, van den Doel LR, van Dedem GW (2005) Quantitative analysis in nanoliter wells by prefilling of wells using electrospray deposition followed by sample introduction with a coverslip method. Anal Chem 77:225–231

Morisset D, Dobnik D, Hamels S, Zel J, Gruden K (2008) NAIMA: target amplification strategy allowing quantitative on-chip detection of GMOs. Nucleic Acids Res 36:e118

Namasivayam V, Larson RG, Burke DT, Burns MA (2003) Transpiration-based micropump for delivering continuous ultra-low flow rates. J Micromech Microeng 13:261–271

Neugebauer S, Evans SR, Aguilar ZP, Mosbach M, Fritsch I, Schuhmann W (2004) Analysis in ultrasmall volumes: micro-dispensing of picoliter droplets and analysis without protection from evaporation. Anal Chem 76:458–463

Neuzil P, Zhang CY, Pipper J, Oh S, Zhuo L (2006) Ultra fast miniaturized real-time PCR: 40 cycles in less than six minutes. Nucleic Acids Res 34:e77

Oh KW, Park C, Namkoong K, Kim J, Ock KS, Kim S, Kim YA, Cho YK, Ko C (2005) World-to-chip microfluidic interface with built-in valves for multichamber chip-based PCR assays. Lab Chip 5:845–850

Pal R, Yang M, Lin R, Johnson BN, Srivastava N, Razzacki SZ, Chomistek KJ, Heldsinger DC, Haque RM, Ugaz VM, Thwar PK, Chen Z, Alfano K, Yim MB, Krishnan M, Fuller AO, Larson RG, Burke DT, Burns MA (2005) An integrated microfluidic device for influenza and other genetic analyses. Lab Chip 5:1024–1032

Pilarski PM, Adamia S, Backhouse CJ (2005) An adaptable microvalving system for on-chip polymerase chain reactions. J Immunol Methods 305:48–58

Prakash AR, Adamia S, Sieben V, Pilarski P, Pilarski LM, Backhouse CJ (2006) Small volume PCR in PDMS biochips with integrated fluid control and vapour barrier. Sens Actuators B 113:398–409

Saiki RK, Scharf F, Faloona F, Mullis KB, Horn GT, Erlich HA, Arnheim N (1985) Enzymatic amplification of beta-globin genomic sequences and restriction site analysis for diagnosis of sickle cell anemia. Science 230:1350–1354

Sista R, Hua Z, Thwar P, Sudarsan A, Srinivasan V, Eckhardt A, Pollack M, Pamula V (2008) Development of a digital microfluidic platform for point of care testing. Lab Chip 8:2091–2104

Squires TM, Quake SR (2005) Microfluidics: fluid physics at the nanoliter scale. Rev Mod Phys 77:977–1026

Timmer BH, van Delft KM, Olthuis W, Bergveld P, van den Berg A (2003) Micro-evaporation electrolyte concentrator. Sens Actuators B 91:342–346

Toriello NM, Liu CN, Mathies RA (2006) Multichannel reverse transcription-polymerase chain reaction microdevice for rapid gene expression and biomarker analysis. Anal Chem 78:7997–8003

Toriello NM, Douglas ES, Thaitrong N, Hsiao SC, Francis MB, Bertozzi CR, Mathies RA (2008) Integrated microfluidic bioprocessor for single-cell gene expression analysis. Proc Natl Acad Sci USA 105:20173–20178

VanDijken J, Kaigala GV, Lauzon J, Atrazhev A, Adamia S, Taylor BJ, Reiman T, Belch AR, Backhouse CJ, Pilarski LM (2007) Microfluidic chips for detecting the t(4;14) translocation and monitoring disease during treatment using reverse transcriptase-polymerase chain reaction analysis of IgH-MMSET hybrid transcripts. J Mol Diagn 9:358–367

Walker GM, Beebe DJ (2002) An evaporation-based microfluidic sample concentration method. Lab Chip 2:57–61

Wang F, Yang M, Burns MA (2008) Microfabricated valveless devices for thermal bioreactions based on diffusion-limited evaporation. Lab Chip 8:88–97

Xu ZR, Zhong CH, Guan YX, Chen XW, Wang JH, Fang ZL (2008) A microfluidic flow injection system for DNA assay with fluids driven by an on-chip integrated pump based on capillary and evaporation effects. Lab Chip 8:1658–1663

Zhang CS, Xing D (2007) Miniaturized PCR chips for nucleic acid amplification and analysis: latest advances and future trends. Nucleic Acids Res 35(13):4223–4237

Zhang CS, Xing D (2009) Parallel DNA amplification by convective polymerase chain reaction with various annealing temperatures on a thermal gradient device. Anal Biochem 387:102–112

Zhang CS, Xu JL, Ma WL, Zheng WL (2006) PCR microfluidic devices for DNA amplification. Biotechnol Adv 24:243–284

Zhang CS, Xing D, Li YY (2007) Micropumps, microvalves, and micromixers within PCR microfluidic chips: advances and trends. Biotechnol Adv 25:483–514

Zimmermann M, Bentley S, Schmid H, Hunziker P, Delamarche E (2005) Continuous flow in open microfluidics using controlled evaporation. Lab Chip 5:1355–1359